The Estimation of TOA T_B from Aquarius Observations

Frank J. Wentz

1. Introduction

The Aquarius L-band radiometers provide four measurements (v-pol, h-pol, +45°-pol, and – 45°-pol) that are each an integration over the entire antenna pattern and as such contain ocean emissions at every possible incidence angle, possibly some land emission, and of course Faraday rotation. In addition, these measurements are not purely polarized, as their name suggest. Rather, a given measurement contains cross-pol components from the other three. In view of this, this report address the following question:

> *Given these four integrated measurements, how well can we estimate the top-of-the-atmosphere (TOA) purely polarized brightness temperature at a constant incidence angle averaged just over the 3-dB footprint?*

The problem is so complex that one must rely on a comprehensive simulation to give the answer.

The calculations reported herein come from an extremely precise integration (about a million integration points per observation). An usually active day for the ionosphere was chosen (Julian day 303 in 2003), and JPL's latest high-density antenna patterns (4 Stokes times 2 ports times 1 million grid points) are used. These integrations provide four polarimetric observations for each horn every 3 seconds along the orbit. A very simple retrieval algorithm is then applied to estimate the purely polarized TOA T_B at a constant incidence angle averaged just over the 3 dB footprint. This retrieval is a critical step in the overall Aquarius retrieval process. It essentially removes all antenna effects and ionospheric effects and provides an earth T_B that just depends on the atmosphere and surface characteristics within the 3-dB field of view.

2. Simulation of Aquarius Observations

Herein, we work in terms of the classical, rather than modified, Stokes parameters. The measurement vector $\boldsymbol{T_A}$, called the antenna temperature vector, is then defined as:

$$\mathbf{T}_A = \begin{bmatrix} T_{Amea,V} + T_{Amea,H} \\ T_{Amea,V} - T_{Amea,H} \\ T_{Amea,+45} - T_{Amea,-45} \\ T_{Amea,left} - T_{Amea,right} \end{bmatrix} \tag{1}$$

Where $T_{Amea,V}$, $T_{Amea,H}$, $T_{Amea,+45}$, and $T_{Amea,-45}$ are the four measurements taken by the Aquarius radiometers. Although there are no Aquarius measurements for the 4th Stokes parameter, $T_{Amea,left}$ and $T_{Amea,right}$, the simulator still computes this quantity.

The measurements represent an integration over the entire 4π steradians surrounding the antenna. We divide this integration into 2 components: the Earth field of view and the space field of view.

$$\mathbf{T_A} = \frac{1}{4\pi}\int_{Earth} \mathbf{G}(\mathbf{b})\,\mathbf{R}(\phi)\,\mathbf{T_B}(\theta_i)\,\frac{\partial\Omega}{\partial A}dA + \frac{1}{4\pi}\int_{Space} \mathbf{G}(\mathbf{b})\,\mathbf{T}_{\mathbf{B},space}\,d\Omega \qquad (2)$$

The first integral is over the surface of the earth, where the differential surface area is dA. The second integral is over space, where $d\Omega$ is the differential solid angle. The other terms in this equation are as follows. The matrix **G** is a 4×4 matrix of the antenna gain function provided by JPL. Each element in this matrix is a function of the look direction **b.** For the first integral, **b** is the unit vector pointing from the antenna to dA. For the second integral, **b** is the unit vector in the direction specified by $d\Omega$.

The term $\mathbf{R}(\phi)$ is a rotation matrix defined by

$$\mathbf{R}(\phi) = \begin{bmatrix} 1 & 0 & 0 & 0 \\ 0 & \cos 2(\phi+\phi_f) & -\sin 2(\phi+\phi_f) & 0 \\ 0 & \sin 2(\phi+\phi_f) & \cos 2(\phi+\phi_f) & 0 \\ 0 & 0 & 0 & 1 \end{bmatrix} \qquad (3)$$

The rotation angle ϕ is an implicit function **b** as well as the attitude of the Aquarius spacecraft. The other rotation angle ϕ_f is the Faraday rotation angle of the ionosphere. It is an implicit function of **b** as well as the Earth's magnetic field vector and the electron density along the path **b** (see equation 7 below). The ratio of the differential solid angle to the differential surface area is

$$\frac{\partial\Omega}{\partial A} = f_{lat}\,\frac{\cos\theta_i}{R^2} \qquad (4)$$

For a spherical Earth, the leading term f_{lat} would be unity. However, the Earth is modeled as an oblate spheroid and as a consequence this term is a function of latitude, deviating about ±1% from unity.

The brightness temperature vectors for Earth and space are

$$\mathbf{T_B}(\theta_i) = \begin{bmatrix} T_{BV}(\theta_i) + T_{BH}(\theta_i) \\ T_{BV}(\theta_i) - T_{BH}(\theta_i) \\ 0 \\ 0 \end{bmatrix} \qquad (5)$$

$$\mathbf{T}_{\mathbf{B},space} = \begin{bmatrix} 2T_{Bspace} \\ 0 \\ 0 \\ 0 \end{bmatrix} \qquad (6)$$

Where T_{BV} and T_{BH} are the v-pol and h-pol Earth brightness temperatures measured at the top of the atmosphere (TOA), but below the ionosphere. They are functions of the Earth incidence angle θ_i at the point where the look vector **b** intersects Earth surface as well as the surface characteristics at dA and the atmospheric absorption and emission along **b**. We have assumed that the 3rd and 4th Stokes parameters coming from the Earth are negligibly small. The term T_{Bspace} is the combined galactic and cosmic brightness temperature, which we assume to be unpolarized.

In doing the Earth integration we use a very fine grid over the antenna's mainlobe, which is defined as 2.5 times the full 3-db beamwidth. Over the mainlobe, dA corresponds to an Earth pixel that is 0.003086^o wide in both latitude and longitude. This very fine spacing for dA is to ensure that the numerical accuracy of the integration over the mainlobe is 0.01%, or better. Outside the mainlobe, dA corresponds to an Earth pixel that is 0.083333^o wide in both latitude and longitude. Because the gain is 30 dB down from its peak value, the integration does not need to be as precise outside the mainlobe.

The percent of power coming from space is about 3 to 4% depending on feedhorn, and the average value of T_{Bspace} is about 3 K. So the contribution of the space integral is about 0.2 K for the first Stokes parameter and 0 for the other 3. We have not actually done the space integral yet, but we are assuming this small term can be estimated with sufficient accuracy so that it will not be a significant source of error. For the results to be presented, we assume the space contribution to $T_{Amea,V}$ + $T_{Amea,H}$ (i.e., the second integral in equation 2) has been exactly calculated and then subtracted out so that the remaining term is just the integral over the Earth.

3. Specifying Earth Surface and Atmosphere for Simulations

This investigation focuses on the retrieval of the TOA Earth brightness temperature. As such, the details of how the Earth surface and atmosphere are specified are not that important. The current methodology for specifying the Earth surface and atmosphere will be made more realistic with time. Pending improvements include using NCEP to model the atmosphere rather than simply using an effective temperature with a constant vapor and cloud content. We also want to implement a more realistic model for land surfaces and include galactic radiation in the downwelling space radiation component. When these more realistic components are implemented, we will repeat the simulations but we do not expect the results reported herein to significantly change because of these updates. Note that the details of the Earth model do matter when one does the next step of converting TOA T_B to salinity. We now described the current models for the Earth surface and atmosphere.

The emission and reflection characteristics of the ocean surface are modeled using Fresnel reflection coefficients for the surface's specular component and the European's Wise model for the wind-induced roughness. The dielectric constant of seawater comes from the Meissner-Wentz (2003) model, which is similar to Klein and Swift. The sea-surface temperature comes from the Reynolds weekly OI product and the wind speed comes from the NCEP 6-hour wind fields. The salinity is simply set to 35 psu for now. For all land surfaces, the emissivity is set to 0.7 and the temperature is set to 288 K.

We model the atmosphere by assuming an effective temperature for the oxygen absorption that is related to the Reynold's surface temperature. Constant vapor and cloud contents are set at 25 mm and 0.05 mm, respectively. The downwelling space radiation is set to a constant 2.7 K.

4. Specifying the Ionosphere and Faraday Rotation for Simulations

The effective height of ionosphere is assumed to be 420 km and the location of the intersection of the look vector **b** with the 420-km layer is first found. Given this location, the total electron content (TEC) is found from the IRI-2001 model and the magnetic flux vector **B** is found from 9th generation IGRF. Given TEC and the dot product of **B** and **b**, the Faraday rotation angle is computed in degrees to be

$$\phi_f = \frac{1.35493\times 10^{-5}}{\nu^2} N_e \; -\mathbf{b}\cdot\mathbf{B} \; \frac{\partial b}{\partial h} \tag{7}$$

where ν is frequency in GHz, N_e is vertically-integrated electron counts in TEC units, **B** is the Earth's magnetic field vector in nanotesla units, and the last term is the partial derivative of slant range to the vertical height, which converts N_e from a vertically-integrated value to a slant-range integrated value. This calculation is done for every integration point over the Earth integral. For the simulation reported herein, we use Julian day 303 in 2003 to specify N_e. This was an unusually active day in the ionsophere and is considered to be somewhat of a worst case.

5. Definition of TAO T_B

It is important to precisely specify the quantity that one desires to estimate given the Aquarius measurements. The quantity we select is the TOA T_B averaged over the 3-dB footprint. We further specify that when doing the footprint averaging, the incidence angle is held to some constant value $\bar{\theta}_i$. The integral over the 3-db footprint is defined as that part of the Earth integral for which the angle between the boresight look vector $\mathbf{b_0}$ and the look vector **b** is less than 3.07°, 3.17°, and 3.24° for the inner, middle, and outer horns, respectively. To be specific, the TOA T_B is given by

$$\bar{\mathbf{T}}_\mathbf{B} = \frac{\int_{3dB\ footprt} \mathbf{T_B}\ \bar{\theta}_i\ dA}{\int_{3dB\ footprt} dA} \tag{8}$$

Thus the only variability of $\mathbf{T_B}$ within the integral is that due to changes in the surface characteristics (i.e., SST, SSS, or wind) and changes in the atmospheric conditions over the 3-dB footprint. We have some freedom as to our choice for the effective incidence angle $\bar{\theta}_i$. For now, we are setting $\bar{\theta}_i$ to the following value, which is indicative of the gain-weighted average of θ_i over the 3 dB footprint.

$$\bar{\theta}_i = \chi\theta_{i,boresight} \tag{9}$$

where $\theta_{i,boresight}$ is the boresight incidence angle, and χ is 1.00177, 1.00186, 1.00148 for the inner, middle, and outer horns, respectively. This adjustment is so small that it probably is not needed and one could simply use the boresight incidence angle in (8).

6. TOA T_B Retrieval Algorithm

The simulation computes both the measurement $\mathbf{T_A}$ and the desired retrieval $\bar{\mathbf{T}}_{\mathbf{B}}$, and the problem at hand is to estimate $\bar{\mathbf{T}}_{\mathbf{B}}$ given $\mathbf{T_A}$. As a trial algorithm we select a very simple approach. The first step is to remove the effect of polarization rotation due to both Faraday rotation (ϕ_f) and spacecraft attitude rotation (ϕ). This is done as follows:

$$\begin{aligned} T'_{A1} &= T_{A1} \\ T'_{A2} &= \sqrt{T_{A2}^2 + T_{A3}^2} \end{aligned} \tag{10}$$

where the prime symbol indicates the polarization rotation correction has been applied and the rightmost subscript indicates which Stokes parameter (i.e. 1st, 2nd, or 3rd). The 1st Stokes parameter is not affected by rotation and hence needs no correction. The correction to the 2nd Stokes parameter is based on the fact that the sum of the squares of the 2nd and 3rd Stokes parameters is invariant under rotation and also on the assumption that the TOA 3rd Stokes parameter from the Earth is negligibly small.

Next the effects of antenna spillover, cross-polarization leakage, and everything else are assumed to be correctable by applying the following linear transformation.

$$\begin{aligned} \hat{T}_{B1} &= a_{11}T'_{A1} + a_{21}T'_{A2} \\ \hat{T}_{B2} &= a_{12}T'_{A1} + a_{22}T'_{A2} \end{aligned} \tag{11}$$

where the caret symbol denotes these are our estimates for $\bar{T}_{B1}$ and $\bar{T}_{B2}$. Past experience indicates that this type of linear transformation is effective in removing spillover and cross-polarization leakage, and the Appendix herein provides additional support for using (11). However, there is certainly no guarantee that it will work sufficiently accurately for Aquarius considering the fact that the Aquarius 3-dB beamwidth is 6° and the Aquarius accuracy requirements are at the 0.1 K level or better. We must use the simulation to evaluate how well this simple retrieval algorithm works. The four coefficients in (11) are derived from a linear regression of $\hat{T}_{Bi}$ to T'_{Ai} using the values coming from the simulation. A separate set of values is determined for each feedhorn. Table 1 gives the coefficient values. The rows labeled "simulation" in Table 1 give the values for the regression coefficients a_{ij} coming from the simulation. The rows labeled "simple analysis" give values obtained from a simple and more traditional approach as is described in the Appendix.

Table 1. The regression coefficients for the TOA T_B Algorithm

	a_{11}	a_{21}	a_{22}	a_{12}
Inner Horn				
Simulation	1.03129	-0.02561	1.06819	-0.00130
Simple Analysis	1.03096	0.0	1.08049	0.0
Middle Horn				
Simulation	1.03706	-0.02760	1.05585	-0.00197
Simple Analysis	1.03582	0.0	1.10013	0.0
Outer Horn				
Simulation	1.04495	-0.03300	1.06765	-0.00777
Simple Analysis	1.04337	0.0	1.11964	0.0

7. Results from the Simulation

The simulations take a very long time to run due to the fine grids used for the integration. A single 3-GHz processor will process about 2 orbits per day when simulated observations are produced every 3 seconds along the orbit. We have eight 3-GHz processors available for this project, and it took several weeks to complete a full 7-day repeat cycle.

The results are shown in terms of the error in estimating the first two Stokes parameters. These errors are defined as:

$$\Delta T_{B1} = \frac{\hat{T}_{B1} - \overline{T}_{B1}}{2}$$
$$\Delta T_{B2} = \frac{\hat{T}_{B2} - \overline{T}_{B2}}{2} \tag{12}$$

We divide by 2 because of the way the classical Stokes parameters translate into the traditional Stokes parameters. This translation is

$$T_{BV} = \frac{I + Q}{2}$$
$$T_{BH} = \frac{I - Q}{2} \tag{13}$$

where I and Q denote the first and second classical Stokes parameters used herein. Thus errors in v-pol and h-pol T_B are proportional to one half the errors in I and Q.

Figures 1 and 2 shows a global map of the mean value of ΔT_{B1} (1^{st} Stokes) within a 1° latitude-longitude cell for ascending and descending orbit segments, respectively. Land areas are shown as light gray. The ascending and descending maps are similar. Both show land contamination near continental coastlines. Away from the coastlines, the error in retrieving the TAO T_B is fairly small (0.02-0.05 K). Figures 3 and 4 are the same as Figures 1 and 2 except that ΔT_{B2} (2nd Stokes) is shown rather than ΔT_{B1}. In this case there is a difference between the ascending and descending maps. The ascending orbit segments are in the evening during which Faraday rotation effects are more severe than in the morning. This can be seen by the larger error shown in Figure 3 (ascending, evening) than Figure 4 (descending, morning). It is interesting that the 2nd Stokes parameter shows much less land contamination than the 1st Stokes parameter.

The next set of figures (Figure 5 through 8) are the same as the first set except the standard deviations of ΔT_{B1} and ΔT_{B2} within a 1° latitude-longitude cell are shown rather than the means. Since these results are for just one repeat cycle, the observations within a given 1° cell should be similar, and one does not expect the standard deviation to be large except near land. This is indeed the case, with the standard deviation being about 0.01 to 0.04 K.

To examine the effect of land contamination more closely, Figure 1 is redisplayed in Figure 9, this time with a color scale that goes from –1 K to + 1 K. Looking at Figures 1 and 9 suggests that land contamination is of the order of 0.1 K when the cell is about 400 km from land.

Overall statistics are computed for open-ocean observations. Open-ocean observations are defined as observations for which the fractional power of radiation coming from land is less than 0.1%. Figure 10 shows the additional land masking that results from this criteria. A good portion of the land contamination shown in the previous figures is removed by applying this masking, but some land contamination (up to 0.1 K) still remains. The mean error in ΔT_{B1} and ΔT_{B1} for open-ocean conditions is essentially zero because the retrieval algorithm regression coefficients a_{ij} were derived from this same set of observations. The rms error in ΔT_{B1} and ΔT_{B2} for open-ocean conditions is about 0.03 to 0.04 K.

8. Conclusions

Based on JPL's current specification of the Aquarius antenna patterns, we conclude that the TOA T_B can be retrieved to an overall (average of morning and evening) accuracy of 0.04 K in open-ocean conditions. The retrieval error is larger during the evening passes due to the residual error in correcting Faraday rotation, which can be as large at 0.1 K in worst cases. As the footprint approaches land, the retrieval error for the TOA T_B will increase, being about 0.1 K when the footprint is about 400 from land.

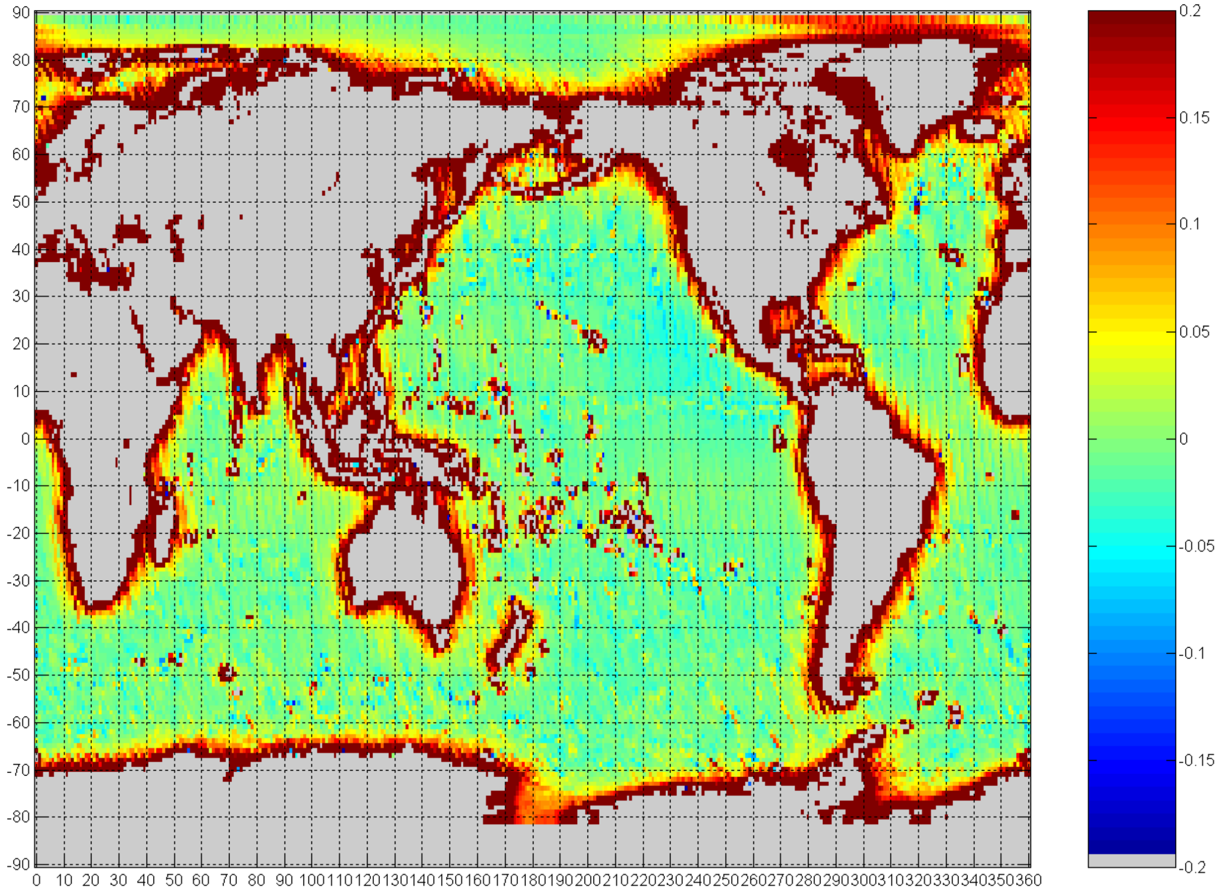

Figure 1. Mean error in retrieving the TOA 1st Stokes parameter for ascending (i.e., local evening) orbit segments. The color scale goes from –0.2 to + 0.2 K and represents ΔT_{B1} (see text).

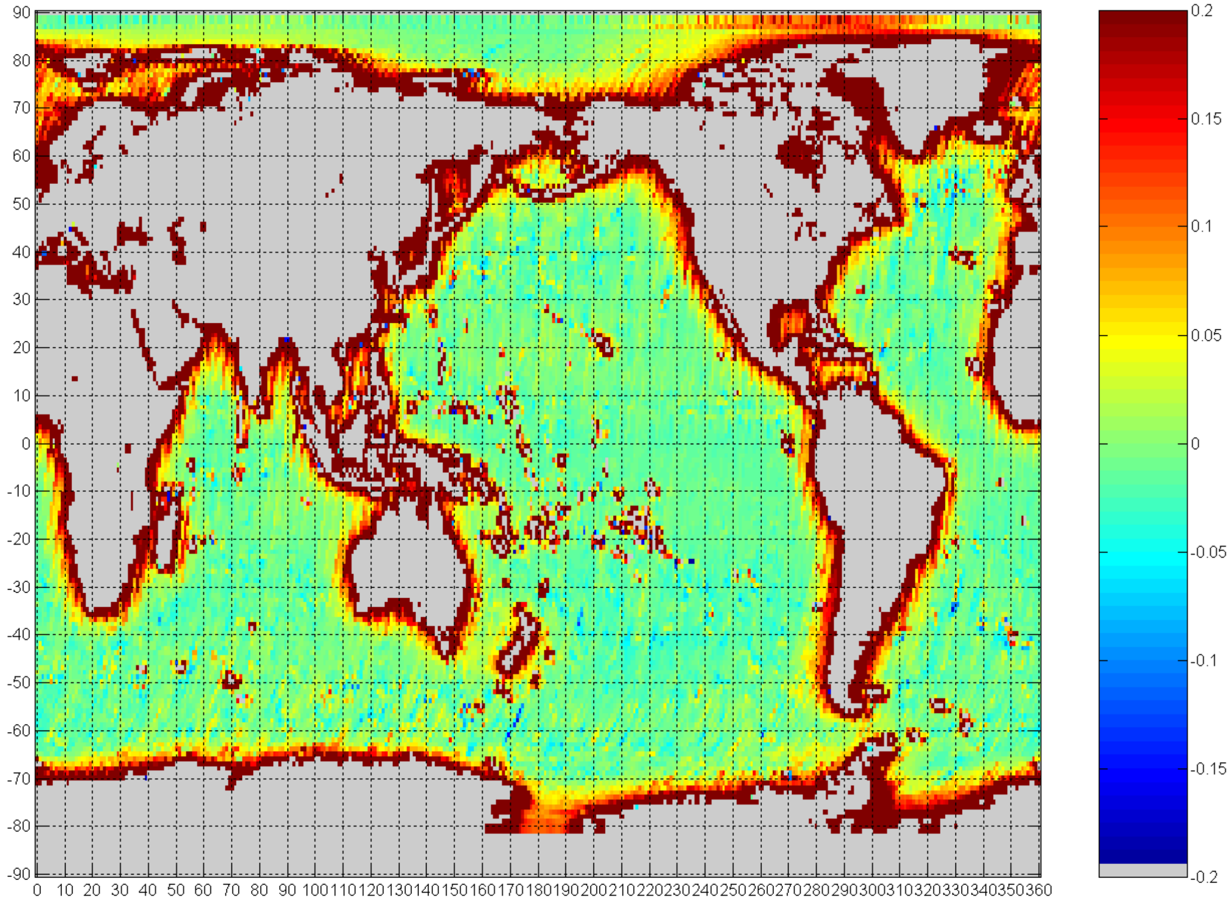

Figure 2. Same as Figure 1 except for descending (i.e., local morning) orbit segments. The color scale goes from –0.2 to + 0.2 K and represents ΔT_{B1} (see text).

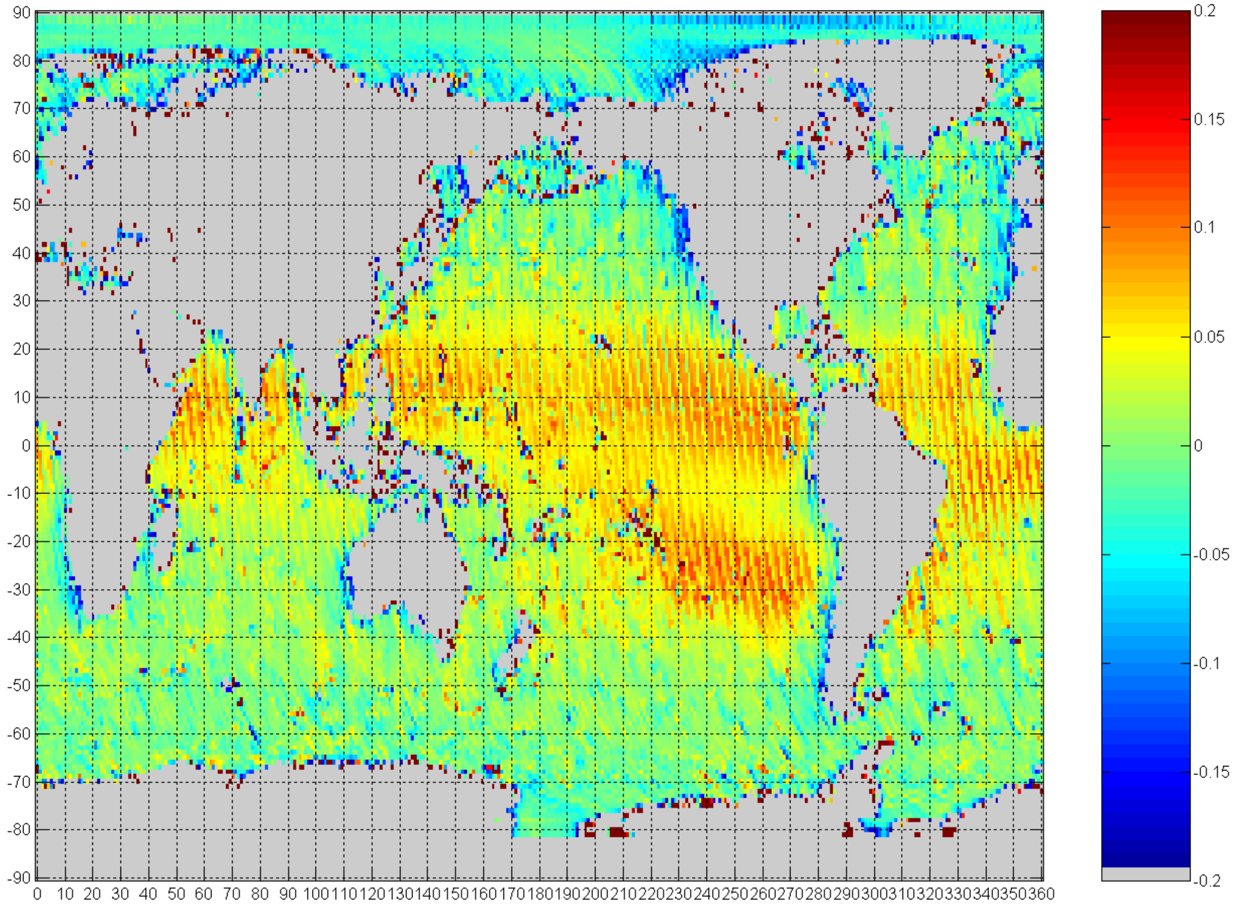

Figure 3. Mean error in retrieving the TOA 2nd Stokes parameter for ascending (i.e., local evening) orbit segments. The color scale goes from –0.2 to + 0.2 K and represents ΔT_{B2} (see text). The red areas are due to Faraday rotation effects not being completely removed.

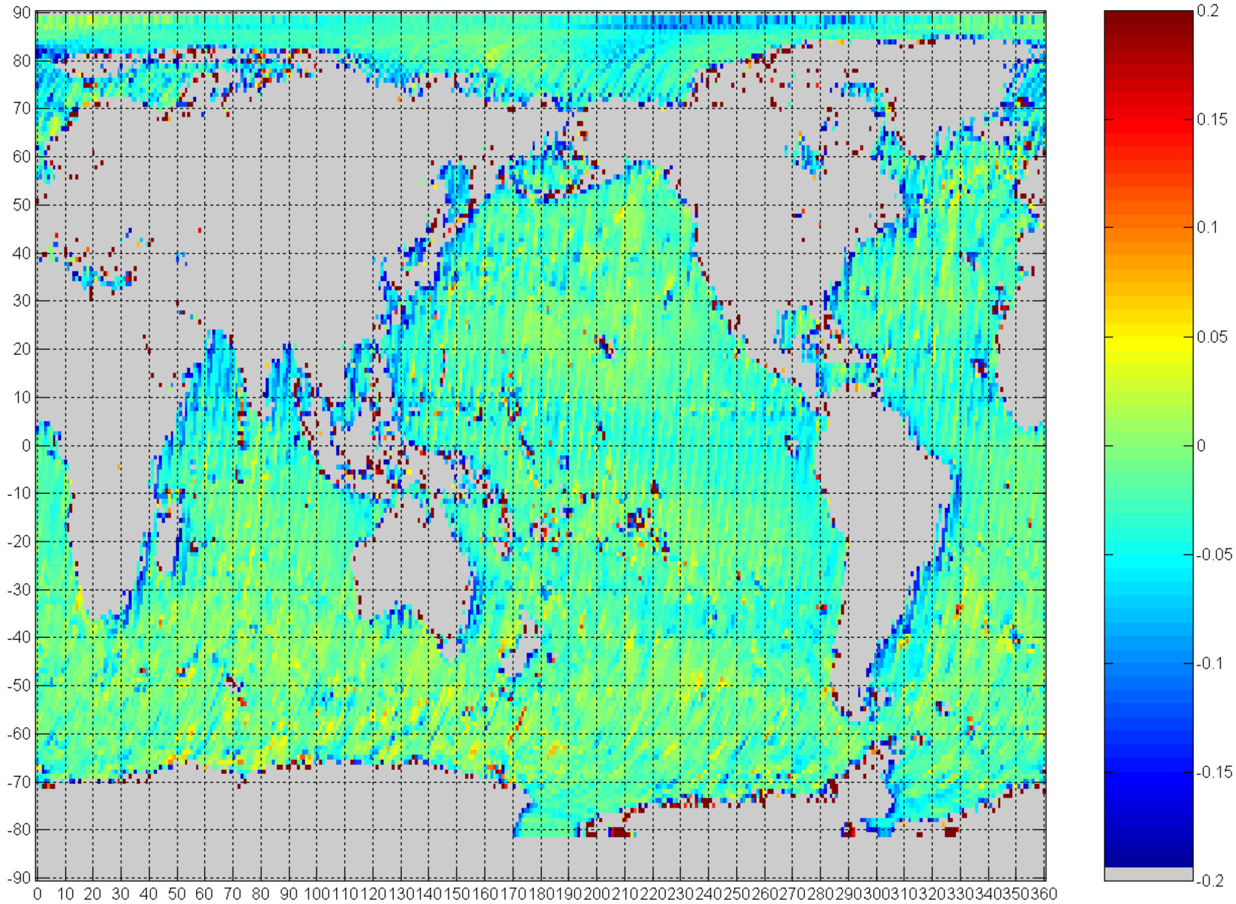

Figure 4. Same as Figure 3 except for descending (i.e., local morning) orbit segments. The color scale goes from –0.2 to + 0.2 K and represents ΔT_{B2} (see text). Faraday rotation effects are much less during these morning orbit segments as compared to the evening orbit segments shown in Figure 3.

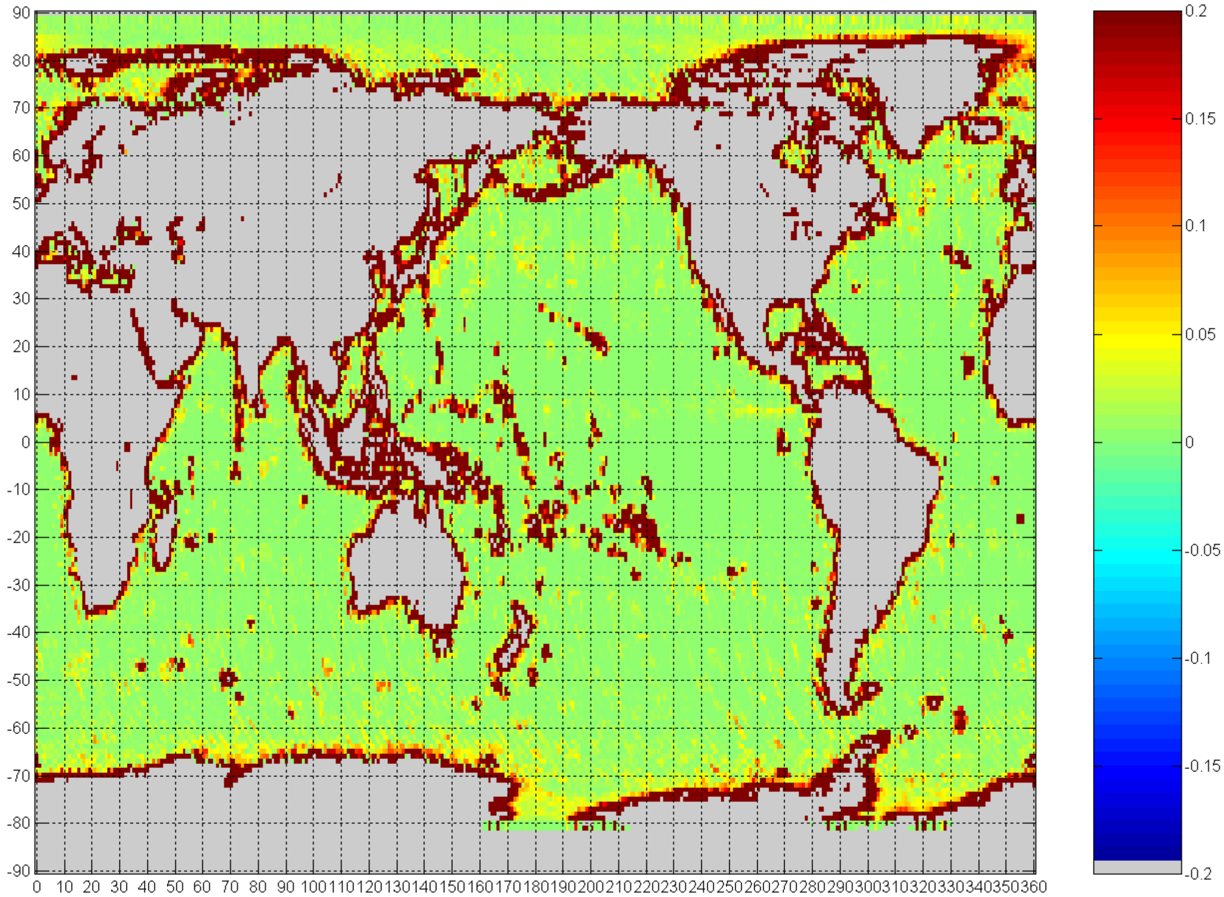

Figure 5. Same as Figure 1 except standard deviation of the error rather than its mean value is shown.

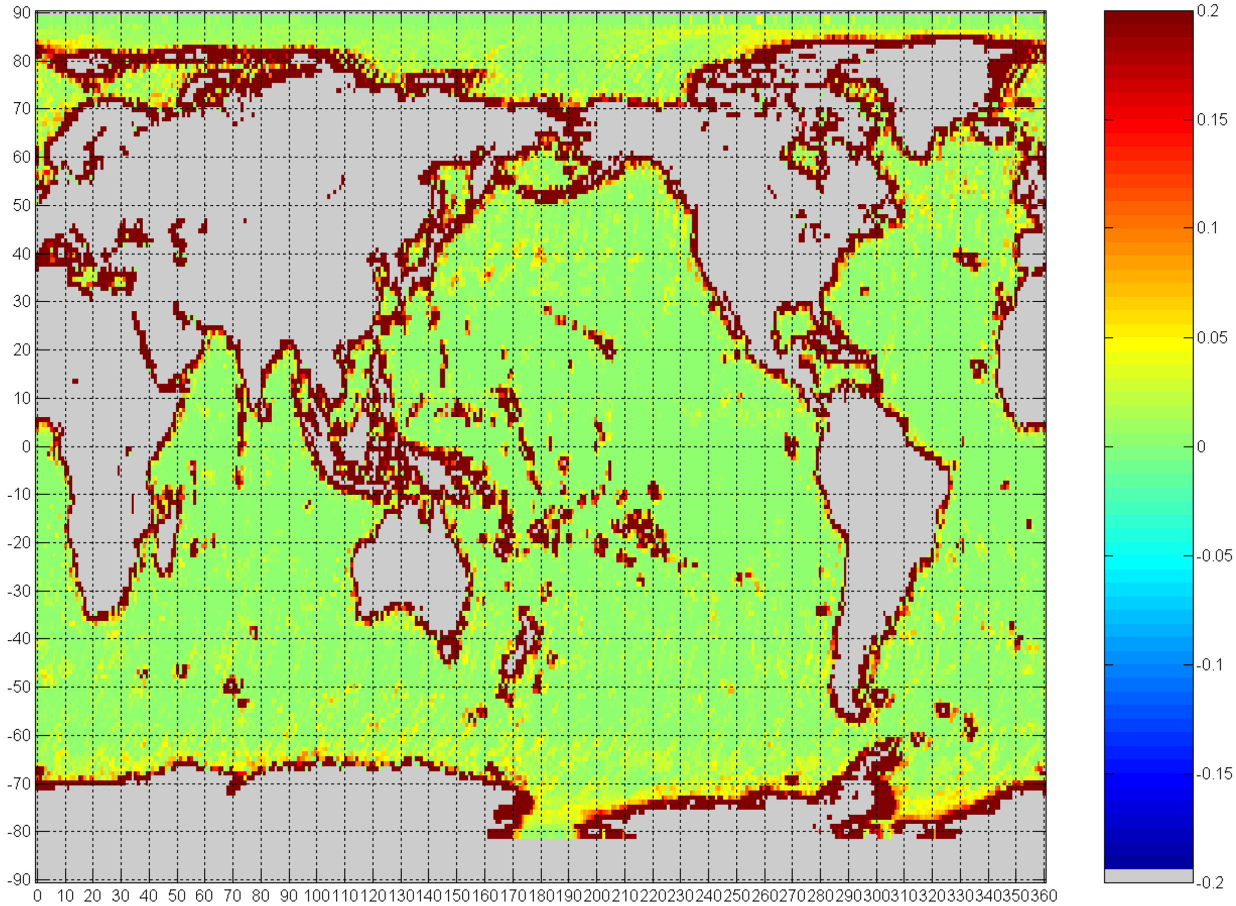

Figure 6. Same as Figure 2 except standard deviation of the error rather than its mean value is shown.

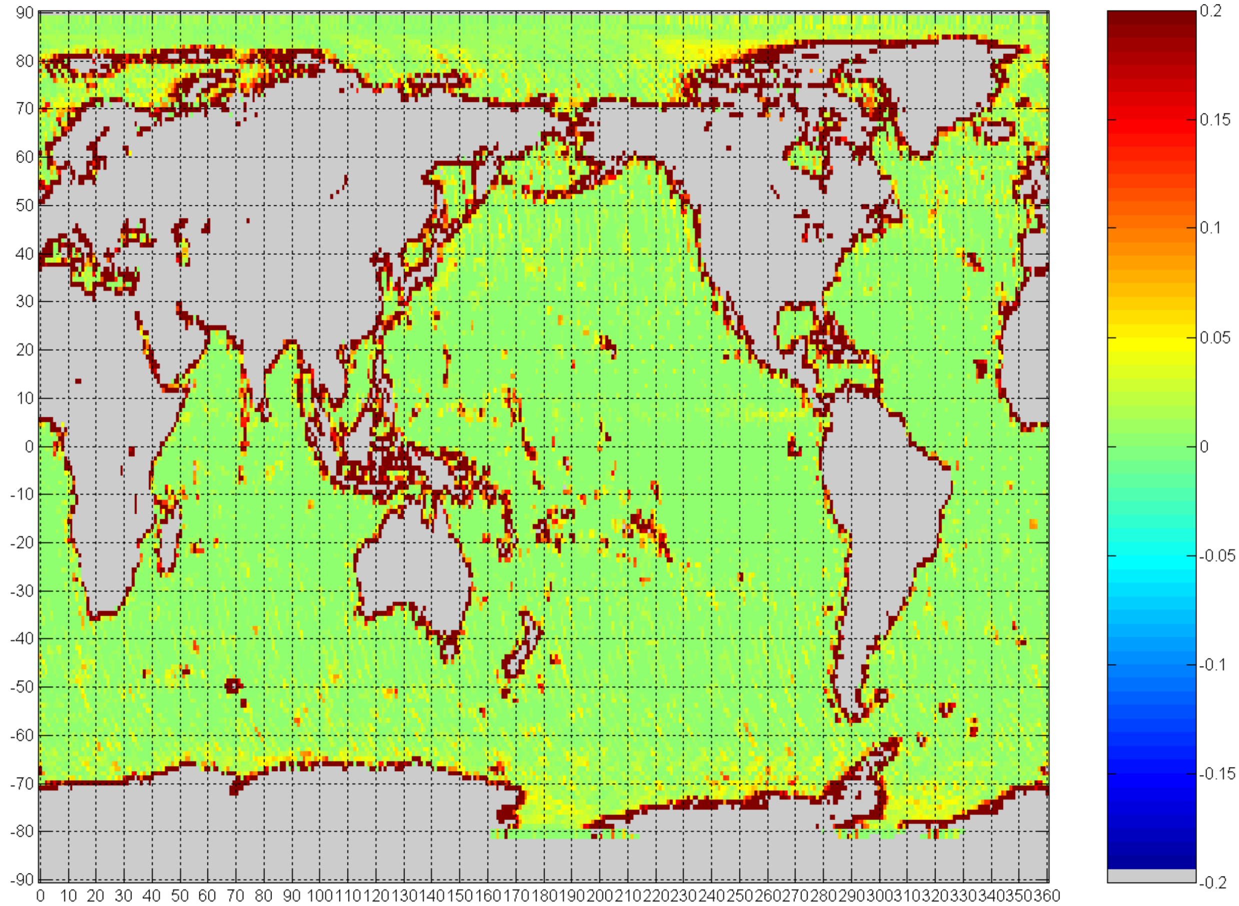

Figure 7. Same as Figure 3 except standard deviation of the error rather than its mean value is shown.

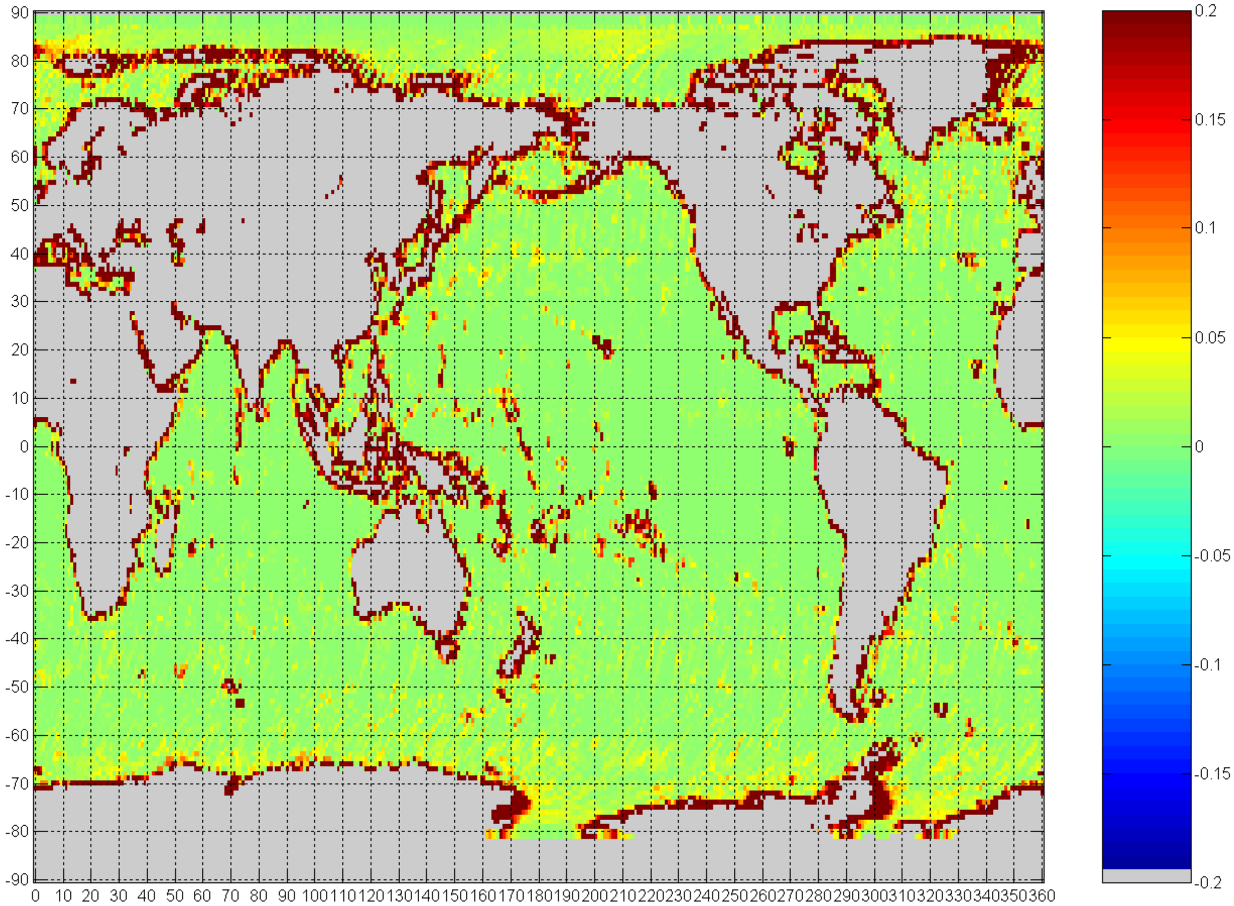

Figure 8. Same as Figure 4 except standard deviation of the error rather than its mean value is shown.

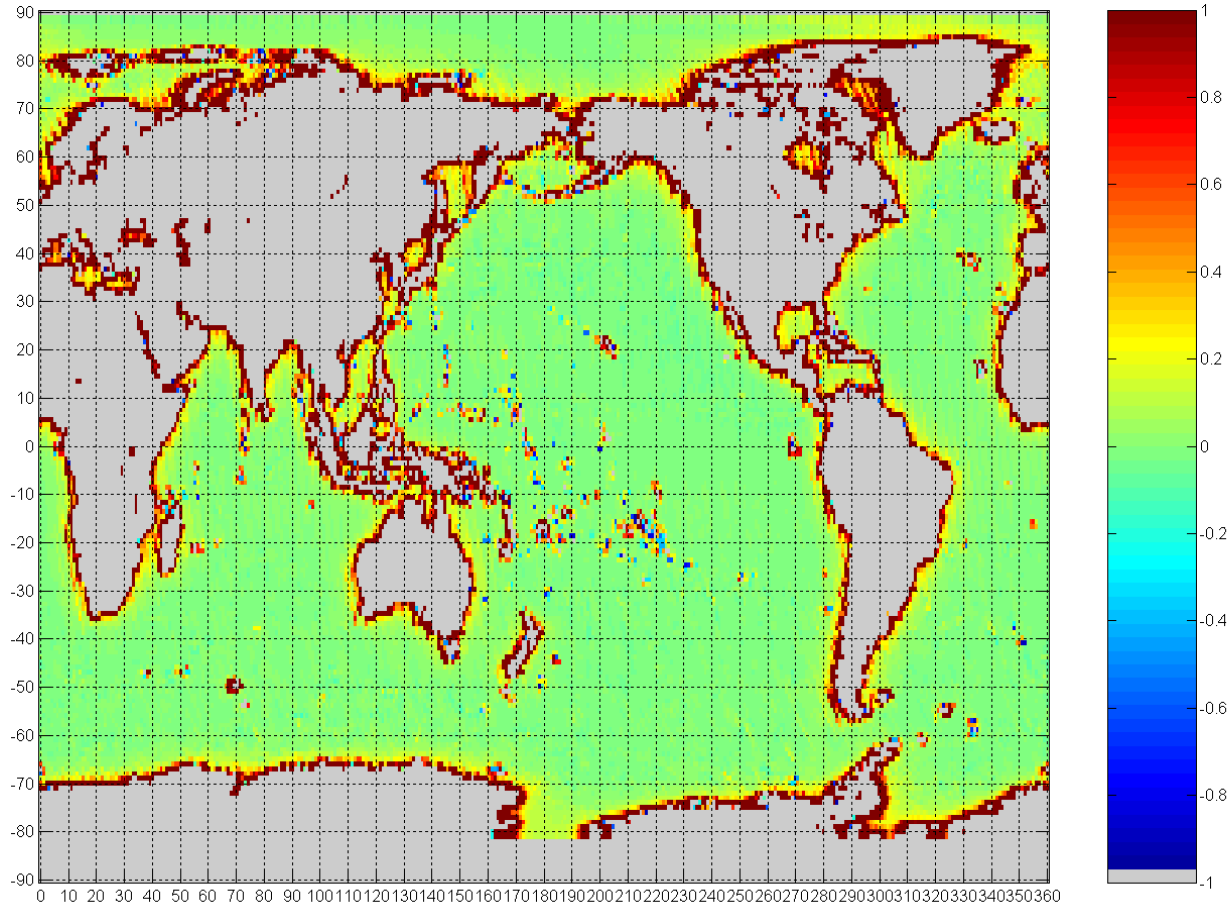

Figure 9 Same as Figure 1 except the color scale is increased to – 1 K to + 1 K.

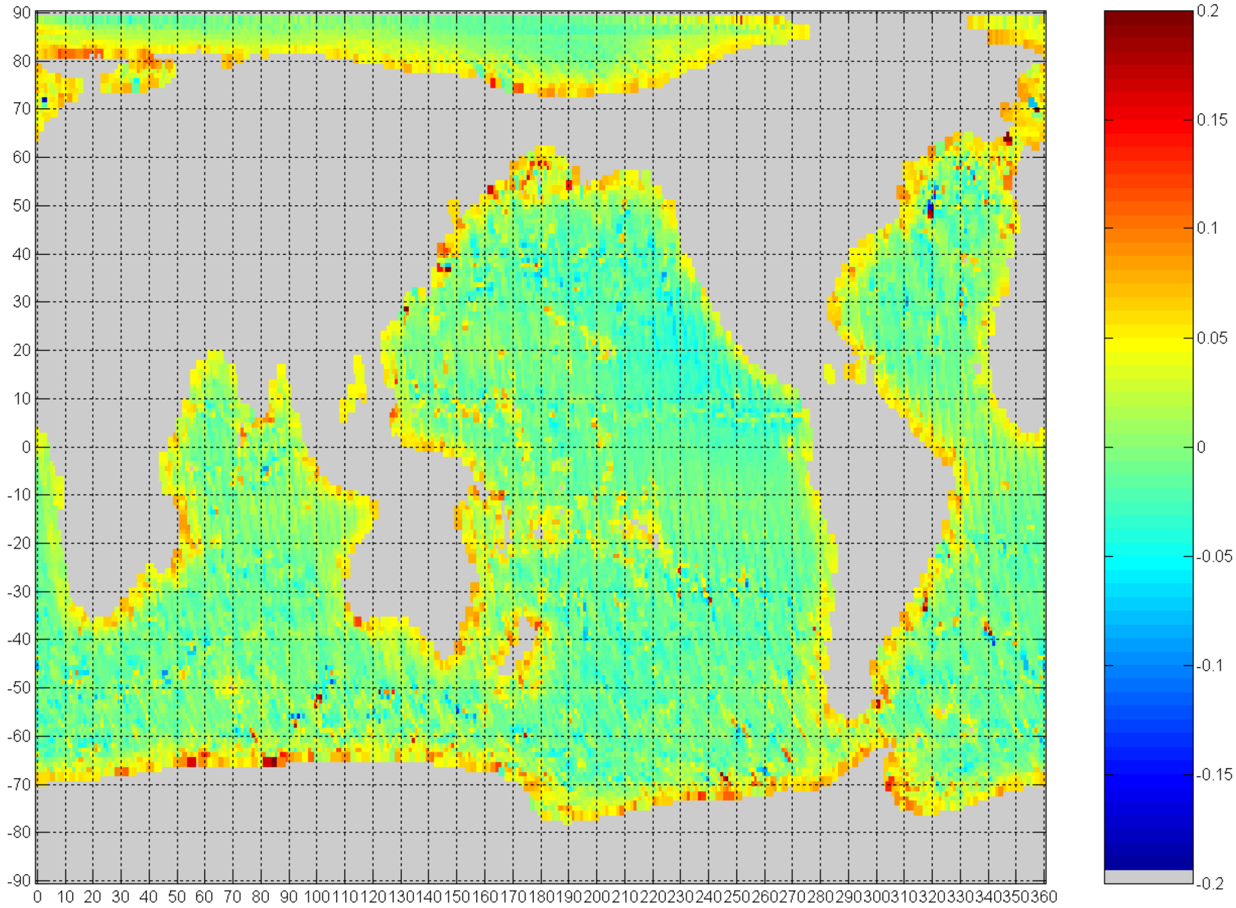

Figure 10. Same as Figure 1 except that an extended land mask is applied. All cells for which the fractional power of radiation coming from land is greater than 0.1% have been masked in the light gray color.

Appendix

A1. Introduction

The purpose of this Appendix is to provide the physical basis for equation (11) and also to provide a consistency check on the value of the a_{ij} coefficients. This Appendix also gives an overview of the commonly used terminology regarding cross-polarization leakage and spillover. This analysis begins by reverting back to the modified Stokes parameters (i.e., v-pol and h-pol) to compute cross-polarization leakage in the traditional way, and then we relate these results to the classical Stokes parameters.

A2. Cross-Polarization Leakage

Each individual element in the 4×4 gain matrix **G** is integrated over the entire 4π steradians surrounding the antenna to obtain:

$$\bar{\mathbf{G}} = \frac{1}{4\pi} \int_{4\pi} \mathbf{G}\ \Omega\ d\Omega \tag{1a}$$

The first and second row of elements in $\bar{\mathbf{G}}$ corresponds to the v-pol and h-pol measurements, respectively. The last two rows correspond to the 3rd and 4th Stokes measurements, respectively. The four columns corresponds to the fractional contribution of v-pol, h-pol, 3rd Stokes and 4th Stokes for the specified measurement. Hence, the off-diagonal terms correspond to cross-polarization leakage. We are using the azimuth-cut gain patterns that have been rotated so that at boresight the v-pol and h-pol antenna polarization vectors are in the plane of incidence and perpendicular to the plane of incidence, respectively.

The gain matrixes $\bar{\mathbf{G}}$ for the three feedhorns are:

$$\bar{\mathbf{G}}_{INNER\ HORN} = \begin{bmatrix} 0.977796 & 0.022204 & 0.000065 & -0.000225 \\ 0.023644 & 0.976356 & 0.000128 & -0.000175 \\ -0.006888 & -0.003493 & 0.889719 & 0.005462 \\ -0.005543 & -0.004798 & -0.007228 & 0.892616 \end{bmatrix} \tag{2a}$$

$$\bar{\mathbf{G}}_{MIDDLE\ HORN} = \begin{bmatrix} 0.969875 & 0.030125 & -0.002784 & -0.001032 \\ 0.028338 & 0.971662 & 0.006321 & -0.000884 \\ 0.013857 & -0.001917 & 0.858496 & -0.006515 \\ 0.023777 & 0.001754 & 0.011222 & 0.860703 \end{bmatrix} \tag{3a}$$

$$\bar{\mathbf{G}}_{OUTER\ HORN} = \begin{bmatrix} 0.965881 & 0.034119 & -0.001427 & 0.000889 \\ 0.033994 & 0.966006 & 0.001721 & -0.000803 \\ -0.014046 & -0.007380 & 0.828256 & 0.001080 \\ 0.014621 & -0.024064 & -0.004273 & 0.830162 \end{bmatrix} \quad (4a)$$

As can be seen, the dominant cross-polarization terms are h-pol leakage into v-pol and v-pol leakage into h-pol, which are highlighted in red. (There are also some relatively large cross-pol terms for the 4th Stokes, but this is of no concern herein.)

The cross-pol leakage is traditionally modeled as:

$$\begin{bmatrix} T_{Av} \\ T_{Ah} \end{bmatrix} = \begin{bmatrix} a_{vv} & a_{hv} \\ a_{vh} & a_{hh} \end{bmatrix} \begin{bmatrix} T_{Bv} \\ T_{Bh} \end{bmatrix} \equiv \mathbf{A} \begin{bmatrix} T_{Bv} \\ T_{Bh} \end{bmatrix} \quad (5a)$$

where the **A** matrix is the upper left four elements in $\bar{\mathbf{G}}$.

The removal of the cross-polarization leakage is done by

$$\begin{bmatrix} T_{Bv} \\ T_{Bh} \end{bmatrix} = \mathbf{A}^{-1} \begin{bmatrix} T_{Av} \\ T_{Ah} \end{bmatrix} \quad (6a)$$

The normalization of antenna pattern requires that a_{vv}+ a_{hv} = a_{hh}+ a_{vh} =1. We also see that the off-diagonal terms are similar in size. Thus a good approximation to (5a) is

$$\begin{aligned} T_{Av} &= T_{Bv} - \varepsilon\ \ T_{Bv} - T_{Bh} \\ T_{Ah} &= T_{Bh} + \varepsilon\ \ T_{Bv} - T_{Bh} \end{aligned} \quad (7a)$$

where $\varepsilon \approx a_{hv} \approx a_{vh}$ is a measure of cross-pol leakage.

An interesting transformation occurs when we switch from the modified Stokes convention to the classical Stokes convention.

$$\begin{aligned} I_{mea} &= T_{Bv} - \varepsilon\ \ T_{Bv} - T_{Bh}\ \ + T_{Bh} + \varepsilon\ \ T_{Bv} - T_{Bh}\ \ = T_{Bv} + T_{Bh} = I \\ Q_{mea} &= T_{Av} - T_{Ah} = T_{Bv} - T_{Bh} - 2\varepsilon\ \ T_{Bv} - T_{Bh}\ \ =\ \ 1 - 2\varepsilon\ \ Q \end{aligned} \quad (8a)$$

Thus in terms of the classical Stokes parameters there is no polarization leakage in the usual sense that we think about it. There is no effect at all on the 1st Stokes parameter, and the 2nd Stokes parameter undergoes a simple scaling, similar to a spillover effect. Thus the cross-polarization analysis is simplified by working in terms of the classical Stokes parameter, which is the convention used in the main body of this report.

A3. Spillover

The measured antenna temperature T_A is given by equation (2) in the main body of this report. When the classical Stokes parameters are used, the required normalization for the antenna pattern is:

$$\frac{1}{4\pi}\int_{4\pi} G_{11}(\mathbf{b})\, d\Omega = 1 \tag{9a}$$

where G_{11} is the first element in the gain matrix $\mathbf{G}(\mathbf{b})$. We now define the following term which is the above integral but just over the Earth field of view.

$$\chi = \frac{1}{4\pi}\int_{Earth} G_{11}(\mathbf{b})\, d\Omega \tag{10a}$$

Spillover can be defined as $1-\chi$, which is the fractional power that comes from space. The on-orbit simulations give the following values for χ: 0.96997, 0.96542, and 0.95843 for the inner, middle and outer horns, respectively.

To see the effect of spillover on the measurement, consider the simple case of the 1st Stokes parameter being at some constant value T_{B1} over the Earth field of view and some other constant value $T_{B1,space}$ over space. Neglecting cross-pol terms, which is a good assumption when working with the 1st Stokes parameter (see above), one obtains

$$T_{A1} = \frac{1}{4\pi}T_{B1}\int_{Earth} G_{11}(\mathbf{b})\, d\Omega + \frac{1}{4\pi}T_{B1,space}\int_{Space} \mathbf{G}(\mathbf{b})\, d\Omega \tag{11a}$$

which can be written as

$$T_{A1} = \chi T_{B1} + (1-\chi)\, T_{B1,space} \tag{12a}$$

The spillover correction is then

$$T_{B1} = \frac{T_{A1} - (1-\chi)\, T_{B1,space}}{\chi} \tag{13a}$$

So the first step in finding T_B given T_A is to estimate the space contribution and then subtract it from the measurement. The second step is to divide by χ.

An analogous derivation can be done for the 2nd Stokes parameter, but in this case the space contribution is zero. One obtains

$$T_{B2} = \frac{T_{A2}}{\chi} \tag{14a}$$

Combining the spillover and the cross-pol corrections given by (8a), one obtains

$$T_{B1} = \frac{T_{A1} - (1-\chi)\, T_{B1,space}}{\chi} \tag{15a}$$

$$T_{B2} = \frac{T_{A2}}{\chi(1-2\varepsilon)} \tag{16a}$$

Thus this analysis suggests that the correction does not involve any cross-pol terms when one works in terms of the classical Stokes parameters. Apart from the subtraction of the cold space term, the only required correction is a multiplicative one.

The major flaw in this simple analysis is the assumption that the brightness temperature stays constant over the Earth field of view. This is of course not the case, particularly for the 2nd

Stokes parameter. However, one might expect that the form for the above correction is appropriate, i.e., a simply multiplicative correction. This hypothesis is tested via on-orbit simulations.

The simulation finds a purely empirical correction of the form given by equation (11). We have assumed space correction is already removed, and hence comparing equation (11) with equations (15a) and (16a), one obtains the following relationships.

$$
\begin{aligned}
a_{11} &= \frac{1}{\chi} \\
a_{22} &= \frac{1}{\chi \;\; 1-2\varepsilon} \\
a_{21} &= a_{12} = 0
\end{aligned}
\qquad (17a)
$$

Table 1 in the main body of this report gives the value of a_{ij} computed from equation (17a). Table 1 also gives the values of a_{ij} coming from the on-orbit simulator. The a_{11} term coming from the simulation is very close to the results coming from (17a) probably because the assumption that the first Stokes parameter is constant over the Earth field of view is a good one. The same is not true for a_{22}, for which the simulation value is considerably less than that from the simple analysis, particularly at the higher incidence angles. The reason for this is probably that much of the field of view outside the antenna's mainlobe comes from the nadir region where the 2nd Stokes parameter is small. Thus the measurement is biased low due to this effect and the correction does not need to be as large as the simple analysis suggests. It is not immediately clear why the simulation yields non-zero values for the cross-pol terms a_{12} and a_{21}, but the values are fairly small anyway.